



Advanced Composite Materials

Publication details, including instructions for authors and subscription information:

<http://www.tandfonline.com/loi/tacm20>

Numerical analysis of heat conduction effect corresponding to infrared stress measurements in multi-lamina CFRP plates

Sunao Sugimoto ^a & Takashi Ishikawa ^b

^a Composite Structure Section, Airframe Division, National Aerospace Laboratory, 6-13-1, Ohsawa, Mitaka, Tokyo 181-0015, Japan

^b Composite Structure Section, Airframe Division, National Aerospace Laboratory, 6-13-1, Ohsawa, Mitaka, Tokyo 181-0015, Japan

Version of record first published: 02 Apr 2012.

To cite this article: Sunao Sugimoto & Takashi Ishikawa (1999): Numerical analysis of heat conduction effect corresponding to infrared stress measurements in multi-lamina CFRP plates, *Advanced Composite Materials*, 8:3, 269-279

To link to this article: <http://dx.doi.org/10.1163/156855199X00263>

PLEASE SCROLL DOWN FOR ARTICLE

Full terms and conditions of use: <http://www.tandfonline.com/page/terms-and-conditions>

This article may be used for research, teaching, and private study purposes. Any substantial or systematic reproduction, redistribution, reselling, loan, sub-licensing, systematic supply, or distribution in any form to anyone is expressly forbidden.

The publisher does not give any warranty express or implied or make any representation that the contents will be complete or accurate or up to date. The accuracy of any instructions, formulae, and drug doses should be independently verified with primary sources. The publisher shall not be liable for any loss, actions, claims, proceedings, demand, or costs or damages whatsoever or

howsoever caused arising directly or indirectly in connection with or arising out of the use of this material.

Numerical analysis of heat conduction effect corresponding to infrared stress measurements in multi-lamina CFRP plates

SUNAO SUGIMOTO* and TAKASHI ISHIKAWA

Composite Structure Section, Airframe Division, National Aerospace Laboratory, 6-13-1, Ohsawa, Mitaka, Tokyo 181-0015, Japan

Received 29 July 1998; accepted 16 December 1998

Abstract—In an infrared stress measurement for multi-lamina CFRP, it is important to evaluate the effect of heat conduction from inner layers induced by the thermoelastic effect. Although a temperature amplitude at a specimen surface is measured in the infrared stress graphic system, the heat flux from the inner layers influences the surface temperature state because it has the same frequency as the applied loads. As a preliminary step of analysis, thermoelastic coefficients of unidirectional CFRP were investigated first. Then, the effects of heat conduction were evaluated numerically for two stacking sequences of CFRP laminates based on an analytical equation and finite element analysis. These calculated results were compared with the experimental results. Two kinds of theoretical results, analytical and finite element analysis, agreed well with experimental results. It was clearly indicated that the thermal conduction must be considered for the infrared stress measurement of multi-lamina CFRP.

Keywords: Thermoelastic constant; thermal expansion; infrared stress measurement; unsteady heat conduction; carbon-epoxy.

1. INTRODUCTION

The infrared stress measurement method presents two advantages among several non-destructive evaluation methods suitable for composite materials: One point is non-contact with the material and the other is intrinsic *in situ* observation. The authors demonstrated in a previous paper [1] that quantitative infrared stress measurement could be performed for a unidirectional carbon fiber-reinforced plastic (UD-CFRP). This work will be briefly reviewed in this paper. In addition, a consideration of the heat conduction from inner laminae was introduced into

*E-mail: sugimoto@nal.go.jp, isikawa@nal.go.jp

analysis by the authors, as in [2] and [3]. In order to understand the reason why this consideration is necessary, the actual procedure in the infrared stress measurement should be explained first. The direct data in this measurement method is an accumulated and averaged temperature amplitude at the surface synchronized with the load period. An accumulation of data is done during multiple load periods to improve S/N ratio in the data. By this requirement, an applied load to the specimen should have constant amplitude and frequency. In the meantime, each layer of a CFRP laminate has an individual temperature amplitude because of the difference between the fiber orientation angles in it, if it exists individually as a hypothetical state. Such a temperature amplitude is created by a reversible exothermic reaction. However, this hypothetical situation is not physically allowed because the layers are adhered together and translaminar heat flux with the frequency equal to the load is generated. This heat flux may affect the surface temperature amplitude.

The effect of the heat conduction was evaluated for two kinds of quasi-isotropic laminates by using an analytical equation and a finite element analysis (FEA). A comparison of the prediction with experimental results was also carried out. In the authors' previous reports, [2] and [3], the quoted value of thermal conductivity from [4] has been used for the analysis. In order to overcome this insufficiency, thermal conductivity was experimentally obtained in this paper by using the steady state heat conductivity measurement method.

2. THERMOELASTIC COEFFICIENTS OF UNIDIRECTIONAL CFRP

It is commonly known that a temperature change is caused by pressure variation in gaseous media under adiabatic conditions. In parallel to gas, it is also caused by stress in solid continua. However, since the temperature change is often very small in the case of a solid, it cannot be observed easily. The temperature change phenomenon by stress in an elastic body under adiabatic conditions is referred to as the thermoelastic effect in this paper. It is reasonably considered that the temperature change is a reversible process and is a basically different phenomenon from an irreversible temperature change such as visco-elastic behavior or internal friction. It is well examined and verified that the temperature change, dT , becomes proportional to the sum of principal stresses on the surface in an isotropic body. However, in an orthotropic body like CFRP, the basic constitutive equations and coefficients appearing in them have to be examined.

If the specimen is a UD-CFRP, the temperature amplitude in the specimen surface is a total of the temperature change by the thermoelastic effect of each stress in the material principal axis. This situation can be written by the following equation, which was introduced by Kageyama *et al.* in a plane stress condition [5].

$$dT = -T(K_L \cdot d\sigma_L + K_T \cdot d\sigma_T), \quad (1)$$

where dT is the temperature amplitude, T is the environmental temperature (in Kelvin), K is the thermoelastic coefficient (TEC), $d\sigma$ is the cyclic stress amplitude, and subscripts L and T denote longitudinal and transverse directions.

K_L and K_T are indicated as follows:

$$K_L = \frac{\alpha_L}{\rho \cdot C_\sigma}, \quad (2)$$

$$K_T = \frac{\alpha_T}{\rho \cdot C_\sigma}, \quad (3)$$

where α is the coefficient of thermal expansion (CTE), ρ is the density, and C_σ the specific heat at constant stress.

Because the TEC in the transverse direction is much larger than in the longitudinal direction, owing to the unique anisotropic CTE property of CFRP lamina [6], the total of the temperature amplitude dT is approximated as the temperature amplitude, dT_T , by transverse stress, if the fiber angle is sufficiently different from zero.

$$dT \cong -K_T \cdot T \cdot d\sigma_T. \quad (4)$$

TECs of the UD-CFRP which were acquired as follows in Refs. [1] and [7] through an infrared stress graphic system (ISGS), JTG-8000 by JEOL Co. Ltd., Japan, will be used in this paper.

$$K_L = -1.21 \times 10^{-13} [1/\text{Pa}], \quad (5)$$

$$K_T = 2.30 \times 10^{-11} [1/\text{Pa}]. \quad (6)$$

These data were modified from raw data by using an emissivity value of 0.96 [8] for black paint for coating to enhance radiation in the specimen surface.

The TECs were also theoretically calculated by using equations (2) and (3) and experimentally obtained material constants in order to validate the measured TECs by the infrared stress measurement. Table 1 shows measured material properties of UD-CFRP appearing in equations (2) and (3). If we substitute these properties of Table 1 into these equations, we have the following TECs:

$$K_L = -8.35 \times 10^{-14} [1/\text{Pa}], \quad (7)$$

$$K_T = 2.40 \times 10^{-11} [1/\text{Pa}]. \quad (8)$$

It should be noted that the measured value of equation (6) by the present ISGS system is sufficiently close to the alternative experimental value of equation (8) by using equation (3) and constitutive material properties. Although the difference between equations (5) and (7) seems to be relatively large, its significance is not serious if we consider that the absolute values of α_L and K_L are quite small and that they may contain experimental errors. From the above discussions, it can be at least concluded that the K_T obtained by the infrared stress measurement system exhibits high reliability. For quick reference, a comparison between theoretical and experimental K_T 's are visually shown in Fig. 1 where experimental raw data before emissivity calibration is also shown.

Table 1.
Input material properties of CFRP for theoretical predictions

Thickness of 1 ply	0.125 mm
Load frequency	5 Hz
Specific heat ^b	977 J/(kg K)
Density ^b	1569.2 kg/m ³
CTE(α_T) ^b	3.68×10^{-5} (1/K)
CTE(α_L) ^b	-1.28×10^{-7} (1/K)
Thermal conductivity ^{a,b}	0.523 W/(m K)
Thermal diffusivity ^{a,b}	3.41×10^{-7} m ² /s

^a In the transverse direction.
^b Experiment.

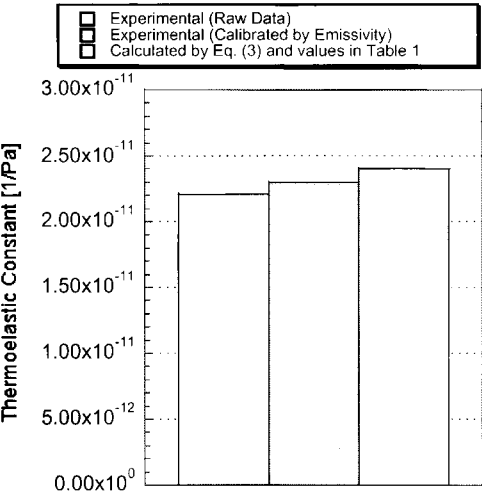


Figure 1. Comparison in transverse thermoelastic coefficients of UD-CFRP.

3. THERMAL CONDUCTIVITY MEASUREMENT OF CFRP BY STEADY STATE METHOD

Preliminary consideration of the thermal conductivity effect was made by the authors [2, 3] based on the quoted transverse conductivity coefficient from other literature [4]. To improve this insufficiency, the thermal conductivity of CFRP was measured by the steady state method here. The used equipment was TCFGM made by DYNATECH Co., USA. The specimen source plate was fabricated with 100 ply unidirectional carbon/epoxy prepreg sheets; T800H/#3631 by Toray Industries Inc., Japan. The specimens were cut out of the plate into a regular dodecagonal shape

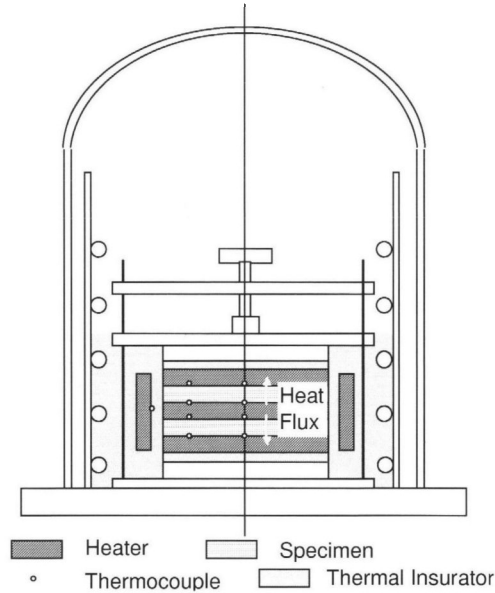


Figure 2. Schematic of thermal conductivity measurement system used here.

with identical side length of 35 mm. A schematic of the measurement system is shown in Fig. 2. A main heater was placed between a set of two specimens in TCFGM and guard heaters were placed above and below the specimens. An outer guard heater of ring shape surrounded around the specimens. Between the outer guard heater and the specimen package, mica flakes were filled for heat insulation. Then electric currents were supplied to the heaters where the current in the main heater was controlled to be a little higher than the guard heaters. Temperatures were measured by thermocouples at each specimen surface after they had reached a steady state. Thermal conductivities were calculated from these temperatures and the differences in electric powers between the main and guard heaters based on a simple one-dimensional heat conduction equation. The measured thermal conductivity in the above-mentioned method is shown in Fig. 3 as temperature dependent values. In the FEA mentioned later, the value of 0.523 W/(m K) obtained at 33°C was adopted.

4. REVIEW OF EXPERIMENTAL SURFACE TEMPERATURE AMPLITUDE FOR TWO QUASI-ISOTROPIC LAMINATES

Previous experimental results of surface temperature amplitude obtained by the authors [9] are shown here again in Fig. 4 for two kinds of quasi-isotropic laminates, A(45): 8 plies, (45/ - 45/0/90)_s, and B(0): 8 plies, (0/90/45/ - 45)_s, fabricated of T400H/#3631 by Toray Industries Inc., Japan. Notations of A(45) and B(0) indicate that the present major concern is placed on the surface 45 and 0 layers

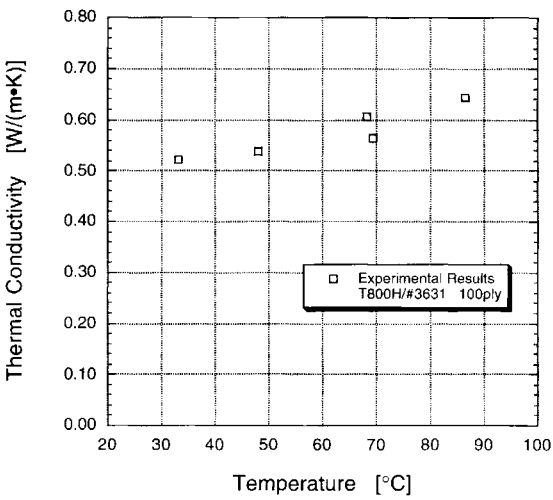


Figure 3. The results of transverse thermal conductivity for T800H/#3631.

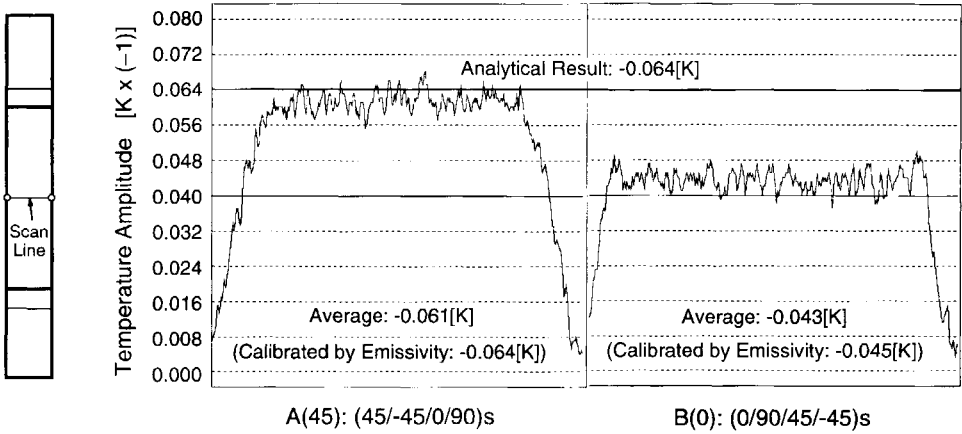


Figure 4. Experimental results of temperature change measured by the ISGS on central scan lines of (45/-45/0/90)_s and (0/90/45/-45)_s specimens.

in two stacking sequences, A and B, respectively. Note that the vertical axis of Fig. 4 is indicated in the reverse scale (toward minus) and that the temperature amplitudes shown in this figure are obtained at the specimen surface, A(45) and B(0), respectively. The applied nominal stress amplitude to both specimens was 90 MPa and this level was determined so as not to induce any damage in the specimens. An average amplitude in a rather uniform distribution portion apart from edges in Fig. 4 left, A(45), indicates -0.061 K. This value is corrected by an emissivity factor of 0.96 for the black paint explained below into -0.064 K. Similarly, a raw average of -0.043 K in Fig. 4 right, B(0), is corrected to -0.045 K.

In order to explain a background of emissivity and radiation, a short note is introduced here. It is indicated in the Stefan–Boltzmann law that infrared radiation

energy on a black body is in proportion to the fourth power of its absolute temperature. In the case of a non-black body, an emissivity should be introduced as a coefficient for describing actual radiation energy. An infrared sensor is based on this relationship to measure the temperature. The specimens used here were always coated with thermal resistance and frosting black paint by Asahi Pen Co. Ltd., in order to enhance infrared emissivity of the surface. Even so, the emissivity of the surface is slightly smaller than the one shown above and its value is available in the theoretical manual [8] of the present infrared camera.

5. PREDICTION BY ANALYTICAL EQUATION

In order to facilitate theoretical prediction of the thermal conductivity effect, two kinds of analysis were conducted: an analytical equation and FEA. Here, the analytical method will be explained first. The following assumptions were introduced not only in the analytical method but also in FEA: (1) The plate is infinite in size. (2) There is an adiabatic wall at the center plane due to a consideration of symmetry. (3) The surface is also assumed as adiabatic by taking the rather high frequency of the load into account. (4) The time considered is infinite to achieve the purely 'repetitive' unsteady state.

The given longitudinal and transverse stresses in each layer were calculated by the laminate theory. Then the temperature amplitude a_j of each layer was calculated. The used material properties in theoretical predictions are shown in Table 1.

An analytical equation used is stated here for predicting the heat conduction effect. This equation is employed after Dunn [4].

$$T(R, t)|_{t \rightarrow \infty} = \frac{1}{2} \sin \omega t \left[\left\{ \sum_{j=1}^{m-1} x_j (a_j - a_{j+1}) \right\} + a_m \right] + \frac{1}{\pi} \left[\sum_{n=1}^{\infty} \frac{(-1)^n}{n} \frac{\sin \omega t + \eta \cos \omega t}{(1 + \eta^2)} \left\{ \sum_{j=1}^{m-1} (a_j - a_{j+1}) \sin x_j n \pi \right\} \right], \quad (9)$$

where R is a half thickness of the specimen, t is the time, $T(R, t)$ is the temperature on R at t , ω is the angular frequency, m is a half of the layer number, x_j is a distance factor from center plane to the surface side in the j th lamina as R is 1, a_j is double the temperature amplitude of the j th layer by the thermoelastic effect, κ is the thermal diffusivity; $\lambda/(\rho C_\sigma)$, η is $\kappa n^2 \pi^2 / (R^2 \omega)$, ρ is density, and C_σ is specific heat under constant stress.

The first remarkable result is that A(45) and B(0) produce the identical temperature amplitude -0.064 K by using equation (9), [2], and [3]. This theoretical prediction and experimental results are compared in Fig. 5 where the raw and corrected experimental data by the emissivity are given for both cases. Simple theoretical predictions are also indicated based on no-heat conduction, i.e. an idea that surface

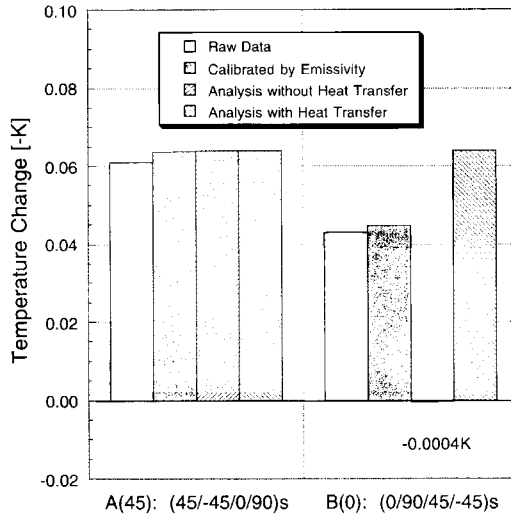


Figure 5. Comparison of temperature amplitude by experiments and analytical equation.

temperature amplitude is deemed a stress and a thermoelastic constant only in the surface layer. Figure 5 shows that a good coincidence is obtained for the A(45) case in comparison with two predictions and the corrected experimental value. It can be concluded that an effect of heat conduction is trivial if the surface layer is highly generating or absorbing heat. However, it indicates a considerable discrepancy between the calibrated experimental (dark column) and theoretical results with heat conduction (hatched column) for the B(0) case. As a statement in the reverse sense, it could be mentioned that a great improvement was obtained if we compare the experimental and theoretical results without heat conduction (small minus value). Based on these findings and incentives, the following FEA has been conducted.

6. PREDICTION BY FEA

The thermal conductivity analysis conducted by the finite element method will be stated in this section. The 2-dimensional 4-node heat conduction element was employed in the FEA software used, MSC/NASTRAN. The analyzed model is shown in Fig. 6. The nodes 51 and 1566 correspond to the surface center of A(45) and B(0) in the experiment, respectively, because all the surrounding walls are assumed to be adiabatic. However, the position in the 0 and 90 layers should be interchangeable in A(45) and B(0). As a heat source in each layer, the heat flux generated by the thermoelastic effect in each layer calculated in the previous section was given at each element. Then the temperature amplitude at time points sufficiently after the start point was obtained at nodes 51 and 1566. The temperature waveforms at these nodes are shown in Fig. 7. Note that the applied load is 5 Hz and that one period should be 0.2 s. These results indicate that these waves have almost reached the regularly sinusoidal state after only a few periods. It is also found in

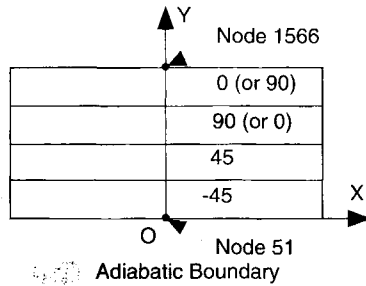


Figure 6. Illustration of the finite element model.

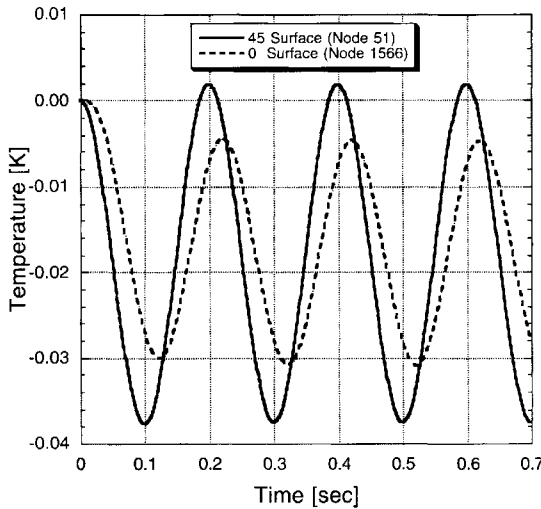


Figure 7. The temperature wave form patterns by FEA.

Fig. 7 that some phase shifts from the applied load occur in 0 and 45 layers and that a shift in the 0 layer is more serious than 45 layer. This finding suggests one of the possible physical mechanisms of ‘phase’ in the present infrared stress measurement. Note that a phase setting should be done in the actual measurement using the present system so as to obtain the maximum temperature amplitude for every specimen.

In order to compare all the experimental and theoretical results, normalizations were done by the amplitude of A(45) in each case and the normalized data are indicated in Fig. 8. A good correlation could be found in the A(45) case as already stated in the previous section. An important improvement in the correlation between theory and experiment was obtained for the B(0) case in Fig. 8 by FEA. This is the most remarkable conclusion of the present paper.

7. CONCLUSIONS

Analytical and finite element predictions were conducted to incorporate thermal conductivity into the problems of infrared stress measurements of two quasi-

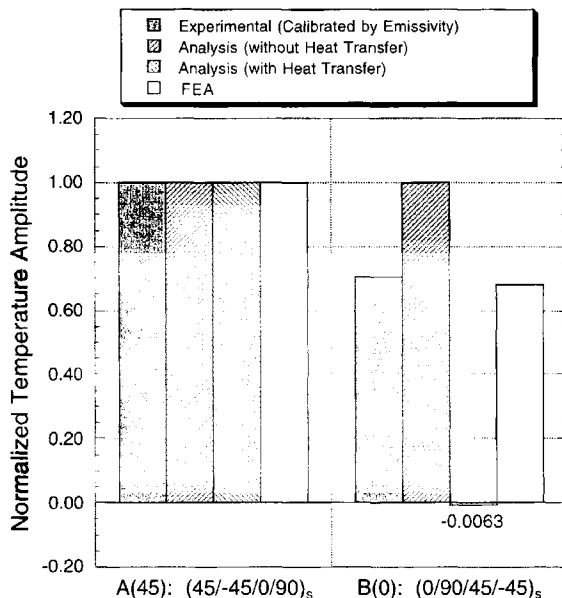


Figure 8. Comparison of the normalized temperature amplitudes by experiments and three theoretical predictions.

isotropic laminates, $(45/-45/0/90)_s$ and $(0/90/45/-45)_s$. The predicted results were compared with the experimental results. It is clarified that the surface temperature of a multi-lamina CFRP is affected by heat conduction from an inner layer heat source and that this effect is enhanced if the surface is a layer of small heat generation. This finding indicates that heat conduction must be considered in infrared stress measurements of such CFRP. Another important finding is that one possible reason of a phase shift in the measurement is heat conduction. In the case of low surface heat generation, the result of the analytical equation is not perfect and the finite element solution provides much better correlation between theory and experiment.

REFERENCES

1. S. Sugimoto and T. Ishikawa, *J. Jpn Soc. Compos. Mater.* **23** (1), 7–14 (1997).
2. S. Sugimoto and T. Ishikawa, in: *Proc. 39th JSASS/SL JSME Struc. Conf.*, pp. 13–16 (1997) (in Japanese).
3. S. Sugimoto and T. Ishikawa, in: *Proc. 22th LSCM Compos. Mater. Symp.*, pp. 92–93 (1997) (in Japanese).
4. S. A. Dunn, *Transaction of the ASME; Series E (J. Appl. Mech.)* **59** (9), 552–558 (1992).
5. K. Kageyama, K. Ueki and M. Kikuchi, in: *Proc. 6th Intern. Congr. Exper. Mech.*, pp. 931–936 (1988).
6. T. Ishikawa, K. Koyama and S. Kobayashi, *J. Compos. Mater.* **12**, 153–168 (1978).
7. S. Sugimoto and T. Ishikawa, in: *Proc. ICCM-11*, Vol. 6, pp. 258–270 (1997) (in Japanese).

8. Jeol Co. Ltd., *The Principle of the Infrared Graphic System: Theoretical Manual* (1988) (in Japanese).
9. S. Sugimoto and S. Ishikawa, in: *Proc. 32nd JSASS Aircraft Symposium*, pp. 71–74 (1996) (in Japanese).